



|                                |   |
|--------------------------------|---|
| <b>Titre:</b><br>Title:        | Flood modelling improvement using automatic calibration of two dimensional river software SRH-2D  |
| <b>Auteurs:</b><br>Authors:    | Simon Deslauriers et Tew-Fik Mahdi  |
| <b>Date:</b>                   | 2018  |
| <b>Type:</b>                   | Article de revue / Journal article  |
| <b>Référence:</b><br>Citation: | Deslauriers, S. & Mahdi, T.-F. (2018). Flood modelling improvement using automatic calibration of two dimensional river software SRH-2D. <i>Natural Hazards</i> , 91(2), p. 697-715. doi: <a href="https://doi.org/10.1007/s11069-017-3150-6">10.1007/s11069-017-3150-6</a> |



### Document en libre accès dans PolyPublie

Open Access document in PolyPublie

|   |   |
|---|---|
| <b>URL de PolyPublie:</b><br>PolyPublie URL:      | <a href="https://publications.polymtl.ca/5331/">https://publications.polymtl.ca/5331/</a> |
| <b>Version:</b>                                   | Version finale avant publication / Accepted version<br>Révisé par les pairs / Refereed    |
| <b>Conditions d'utilisation:</b><br>Terms of Use: | Tous droits réservés / All rights reserved  |



### Document publié chez l'éditeur officiel

Document issued by the official publisher

|   |   |
|---|---|
| <b>Titre de la revue:</b><br>Journal Title: | Natural Hazards (vol. 91, no 2)   |
| <b>Maison d'édition:</b><br>Publisher:      | Springer  |
| <b>URL officiel:</b><br>Official URL:       | <a href="https://doi.org/10.1007/s11069-017-3150-6">https://doi.org/10.1007/s11069-017-3150-6</a>   |
| <b>Mention légale:</b><br>Legal notice:     | This is a post-peer-review, pre-copyedit version of an article published in Natural Hazards. The final authenticated version is available online at:<br><a href="https://doi.org/10.1007/s11069-017-3150-6">https://doi.org/10.1007/s11069-017-3150-6</a> |

**Ce fichier a été téléchargé à partir de PolyPublie,  
le dépôt institutionnel de Polytechnique Montréal**

This file has been downloaded from PolyPublie, the  
institutional repository of Polytechnique Montréal

<http://publications.polymtl.ca>

1                   **Automatic calibration of river reach 2D simulations based on SRH-2D**

2   Simon Deslauriers<sup>1</sup>, Tew-Fik Mahdi<sup>2</sup>

3   <sup>1</sup>Département des génies Civil, Géologique et des Mines (CGM), École Polytechnique de  
4   Montréal, C.P. 6079, succursale Centre-Ville, Montréal, QC H3C 3A7, Canada. Email:  
5   simon.deslauriers@polymtl.ca

6   <sup>2</sup> Professor, Département des génies Civil, Géologique et des Mines (CGM), École  
7   Polytechnique de Montréal, C.P. 6079, succursale Centre-Ville, Montréal, QC H3C 3A7,  
8   Canada (Corresponding author). Email: [tewfik.mahdi@polymtl.ca](mailto:tewfik.mahdi@polymtl.ca)

9   Word count: 6 784

10 **ABSTRACT**

11 River model calibration is essential for reliable model prediction. The manual calibration  
12 method is laborious and time consuming and requires expert knowledge. River  
13 engineering software is now equipped with more complex tools that require a high  
14 number of parameters as input, rendering the task of model calibration even more  
15 difficult. This paper presents the calibration tool O.P.P.S. (Optimisation Program for  
16 PEST and SRH-2D), then uses it in multiple calibration scenarios. O.P.P.S. combines PEST,  
17 a calibration software, and SRH-2D, a bi-dimensional hydraulic and sediment model for  
18 river systems, into an easy-to-use set of forms. O.P.P.S is designed to minimize the  
19 user's interaction with the involved program to carry out rapid and functional  
20 calibration processes. PEST uses the Gauss-Marquardt-Lavenberg algorithm to adjust  
21 the model's parameters by minimizing an objective function containing the differences  
22 between field observation and model-generated values. The tool is used to conduct  
23 multiple calibration series of the modelled Ha! Ha! river in Québec, with varying  
24 information content in the observation fields. A sensitivity study is also conducted to  
25 assess the behaviour of the calibration process in the presence of erroneous or  
26 imprecise measurements.

27 **Keywords:** river modelling; automatic calibration; parameter estimation; SRH-2D; PEST

28

## 29 **1 Introduction**

30 River models are used in various ways by engineers in many fields. These models are  
31 relied upon to assess problems that cannot be studied directly or that are too complex  
32 to be addressed via simplified approaches. River models are generally oriented towards  
33 predictions in many environmentally oriented fields of study, such as water quality,  
34 flood prediction and sediment transport.

35 In most study cases, the process of building a functional model comprises four main  
36 steps (Vidal et al., 2007): model set-up, model calibration, model validation and  
37 exploitation. Model calibration, being an essential and crucial step, consists of the  
38 adjustment of the model's parameters until a satisfactory agreement between  
39 simulated values and measured values is obtained. Hydraulic models include a certain  
40 variety of parameters that cannot be measured or assessed via field measurements or  
41 observations. Reliable model predictions will therefore be obtained through a thorough  
42 calibration process (Bahremand & De Smedt, 2010).

43 The manual calibration task is commonly performed in a trial and error process where  
44 the user progressively adjusts the parameters until a satisfactory result is obtained. This  
45 method is limited since the task is time consuming and the subjectivity of the quality of  
46 the adjustment highly depends on the user's experience (Boyle et al., 2000). Moreover,  
47 the number of variable parameters is often reduced as much as possible by the users to  
48 reduce the model's complexity. With the ever-growing computational capabilities of the

49 models and the increasing demand for model precision, the manual calibration method  
50 sometimes becomes inappropriate.

51 Dedicated studies have aimed to develop efficient and automatic calibration methods  
52 where the parameters are adjusted until an objective function is brought to a minimum.

53 Calibration methods come in two forms: the global methods based on an evolution  
54 algorithm, such as the Shuffled-Complex Evolution method (Duan et al., 1992), and the  
55 gradient-based methods, such as the Gauss-Marquardt-Levenberg algorithm. Global  
56 methods are robust in finding the minimum of the objective function in the entire  
57 parameter space but require a great amount of model runs to achieve this result.

58 Gradient-based methods on the other hand are computationally efficient, but the result  
59 can sometimes be dependent on the initial parameters as the calibration progresses  
60 from an initial set of parameters towards the steepest descent of the objective function.

61 Model calibration, regardless of the chosen method , should be done with caution as  
62 multiple parameter sets of model structure could exist and yield equally acceptable  
63 results (Beven & Freer, 2001). The existence of these different possibilities is known as  
64 “equifinality” and has been well documented before (Pathak et al., 2015). The issue of  
65 equifinality is not the main focus of the authors in this study but rather the application  
66 of a “work-around” technique to avoid it.

67 Though the hydraulics models have evolved into complex tools with diverse  
68 functionalities to visualise and present results, calibration-oriented tools have not  
69 progressed in the same manner. Additional features have been implemented in the

70 models to yield more capabilities in data presentation, but little has been done  
71 regarding the improvement of the calibration tools: “evolution of calibration support  
72 mechanisms has yet to undergo the same level of development as the models  
73 themselves” (McKibbon & Mahdi, 2010). Vidal et al. (2007) depicted the same problem:  
74 “even modelling packages promoting good modelling practices do not provide  
75 significant features to assist users during manual calibration”.

76 For the same solver, or software, even if PEST (Parameter ESTimation) can be used to  
77 calibrate a particular river model (Lavoie and Mahdi, 2016), the tedious calibration  
78 process has to be repeated again for a new river model even if using the same solver. To  
79 facilitate the calibration process, an automatic calibration tool is created that combines  
80 PEST and SRH-2D (Sedimentation and River Hydraulics). To the knowledge of the  
81 authors this is the first time that a tool based on PEST is developed to calibrate any river  
82 model based on the SRH2-D, a 2D free hydrodynamics software developed by the USBR  
83 (U.S. Bureau of Reclamation). The user simply specifies the parameters he wishes to  
84 submit to the calibration process and the observation values to be compared with the  
85 simulated results. The developed tool then assures the entire configuration and  
86 execution of the calibration process.

87 The tool created is then used to explore different calibration scenarios where the effect  
88 of progressively increasing the available information used by the calibration process is  
89 considered. Another set of calibrations is undertaken with the introduction of an error

90 in the measurement values to explore the effect of erroneous data. This paper deals  
91 only with the calibration of the Manning's roughness coefficient.

## 92 **2 Methods**

93 This section introduces the hydrodynamic model used for the river reach flow  
94 simulation, SRH-2D, and the optimisation program PEST. The tool developed is also  
95 presented, along with the description of the conducted calibration series on the model.

### 96 **2.1 SRH-2D**

97 SRH-2D (Lai, 2008) is a depth-averaged flow and sediment transport model for river  
98 systems that was developed at the U.S. Bureau of Reclamation. The software is capable  
99 of simulating flow through multiple reaches, floodplains, vegetation lands and  
100 hydraulics structures. SRH-2D is well suited for rivers that require a better  
101 representation of 2D effects, such as multiple flow paths or in-stream structures. It  
102 computes the local water elevation, local flow velocity, eddy pattern and shear stress on  
103 riverbeds and banks. The software is built to easily divide rivers into different reaches  
104 depending on vegetation, topography or morphology. The hybrid meshing strategy is  
105 well suited to zonal modelling as it allows for both a quadrilateral and triangular shape  
106 with the desired density.

107 An implicit scheme is used to solve the finite-volume numerical method based on the 2D  
108 depth average dynamic wave equation of St. Venant. Steady and unsteady state can  
109 both be simulated by the software, and all flow regimes may be simulated. For a better  
110 understanding of the model, additional details can be found in Lai (2009), where a

111 complete description of the governing equation and discretisation methods is displayed.

112 Although SRH-2D is capable of computing sediment transport, this model is considered

113 static and therefore does not include aggradations or degradation of the riverbed.

114 Pre-processing and post-processing of the model is executed in SMS (Aquaveo, 2013), a

115 modelling software presented as a graphical user interface and analysis tool that holds

116 all of the SRH-2D functionalities.

## 117 **2.2 PEST**

118 To verify the reproduction of the physical phenomena by the model, the data calculated

119 by the model needs to be compared with measured values to determine the model's

120 performance regarding the reproduction of the said phenomena. Based upon the

121 assumption that the model responds to an excitation or an impulsion, it is possible to

122 imagine that there is at least a combination of parameters that can make the model

123 reproduce the same reactions that occur in the modelled environment (Doherty, 2010).

124 PEST is a model-independent software designed to assume the task of calibration in a

125 completely automatic manner by applying the Gauss-Marquart-Levenberg algorithm

126 (Doherty, 2010). The calibration is undertaken by reducing to a minimum the objective

127 function, which holds the discrepancies between the measured values and the results

128 given by the model. PEST will gradually adjust the model parameters following the

129 steepest descent towards the minimum of the objective function until it reaches the

130 user-supplied termination criteria. The parameters obtained would hence give the best

131 match between the supplied measured values and the simulated values.



132 The parameter estimation is based on a linearization of the relationship between the  
133 model parameters and the calculated output values. At every iteration, PEST executes as  
134 many model runs as there are calibration parameters to generate their partial  
135 derivatives using a user-guided finite difference. Following every model run, PEST  
136 examines the output information and, based on the instruction supplied in the control  
137 files, will refine the input parameters of the model towards the predicted steepest  
138 descent of the objective function based on the calculation of the Jacobian matrix of the  
139 model parameters. PEST will stop this process once the objective function is reduced to  
140 a minimum.

141 To conduct this task, PEST takes control of the model by executing it as many times as  
142 needed while modifying the parameters until the objective function is lowered to a  
143 user-supplied satisfactory level. PEST requires a specific set of instructions in the form of  
144 three files. The first file indicates the way in which the output information generated by  
145 the model should be interrogated. The second is a mirror image of the input file, which  
146 is used to locate the calibration parameters. The third file is the centre of command of  
147 the whole operation and contains all the instructions regarding the calibration process  
148 (Doherty, 2010). The content of these files will vary from one model to another.

149 In this unique approach, PEST is linkable to almost any type of model as long as the  
150 input and output information can be accessed in any way. The sequential execution of  
151 the model by PEST is accomplished via a batch file, which can be a succession of multiple  
152 operations such as the translation of the output file to a readable format or the

153 combination of multiple information coming from the model resolution. PEST has  
154 already been proven to be an effective calibration procedure for hydrological models  
155 and quasi-2d hydrodynamic models (Diaz-Ramirez et al., 2012; Ellis et al., 2009; Fabio et  
156 al., 2010; Kim et al., 2007; McCloskey at al., 2011; McKibbon & Mahdi, 2010; Rodeetal.,  
157 2007)

### 158 **2.3 O.P.P.S.**

159 The Optimisation Program by PEST for SRH-2D (O.P.P.S.) is the resulting tool for the  
160 automatic calibration of SRH-2D by PEST. O.P.P.S. eases the task of preparing the  
161 calibration process by correctly building the required files with the user's desired PEST  
162 regularisation parameters. O.P.P.S. comes in the form of an easy-to-use graphical  
163 interface based on Excel® Visual Basic, where the user can quickly specify the current  
164 project's parameters to be calibrated and the measured values that are to be matched  
165 in the model.

166 O.P.P.S can easily prepare and execute an operational PEST calibration process with  
167 minimum user interaction. The model is sequentially launched by a command line in the  
168 form of an AutoHotKey® file capable of conducting single model runs without any user  
169 intervention. Indeed, the execution of the command lines supplied with O.P.P.S. allow  
170 for carrying out the calibration process in the background without the user  
171 interventions normally required by SHR-2D. A single non-calibration run would normally  
172 require multiple human-directed operations that would interfere with the automatic

173 aspect of the calibration process. Therefore, the automatic execution of SRH-2D is made  
174 completely free of user interventions.

175 When O.P.P.S. is launched, the interaction with the user is made through a series of  
176 forms in which the information regarding the calibration process can be entered. A  
177 summary of the procedures followed during the preparation and execution of the  
178 calibration process is presented in figure 1. Any combination of measured depth, water  
179 velocity along the X- and Y-axis, and the velocity magnitude at any point in the model  
180 can be supplied as observation values to be compared to the simulated results for each  
181 observation point. The measured values supplied are individually used in the calibration  
182 process: there will be as many single observation points as there are measured values in  
183 the calibration process.

184 The subsequent preparation steps are carried out by O.P.P.S. and the calibration process  
185 is guided by PEST. Once the parameters and the observation points have been  
186 identified, O.P.P.S can create the required files for PEST's execution. A series of  
187 verifications are performed to avoid errors or performance issues that can arise when  
188 PEST is not efficiently programmed. If it does not exist already, O.P.P.S. will  
189 automatically create a backup file of the project. When PEST is executed, permanent  
190 changes will be applied to the selected parameters. Additional options for the fine  
191 tuning of the calibration process are also available.

192

193 Additional parameters can be adjusted for the fine tuning of the calibration process by  
194 managing the evolution of the calibration process.. The user can adjust the Marquardt-  
195 Lambda parameter, which guides the progression vector towards the optimal reduction  
196 of the objective function. The progression vector is gradually reduced as PEST  
197 progresses closer to the minimum of the objective function. PEST is presented with  
198 multiple decision criteria that can be adjusted by the user, depending on the project at  
199 hand. These criteria handle the conditions required to progress towards a new iteration  
200 or to terminate the calibration process at the most appropriate moment. In both cases,  
201 these regularisation parameters can be based on the evolution of the calibration  
202 parameters or on the progression of the objective function. . These parameters should  
203 be adjusted according to each project, as one configuration might not satisfy every  
204 calibration operation.

## 205 **2.4 Study case**

206 O.P.P.S. can quickly and efficiently assemble the required information to perform an  
207 operational automatic calibration process. This tool is used to perform a series of  
208 calibrations of the river model. In this study, the Ha!-Ha! River is partially modelled using  
209 the topographical data collected after the 1996 failure of a dam of the Ha! Ha! Lake. The  
210 dam failed as water rose rapidly during the high-yield rains that lasted for three days in  
211 the Saguenay region in Québec, Canada. The sudden flush caused an excessive increase  
212 in the river flow (more than 1000 m<sup>3</sup>/s), drastically changing the river morphology by  
213 eroding the sediment deposit around the rocky bases of the riverbed. Capart *et al.*  
214 (2007) give the cross-sections data for every 100 m of the river.

215 The Ha! Ha! River basin covers a total of 572 km<sup>2</sup> in the Saguenay-Lac-St-Jean region,  
216 and its river stretches forth a total of 35 km from the Ha!-Ha! dyke to the river mouth,  
217 where it flows into the Saguenay river. The model comprises five different reaches of  
218 approximately 3 km each represented by different roughness coefficients. A map of the  
219 modelled reaches is presented in figure 2. The Manning roughness coefficient is the only  
220 adjustable parameter in the study case as PEST only allows for the calibration of  
221 continuous parameters. Although the calibration is limited to only one parameter, the  
222 roughness coefficient has been identified as the most influential source of uncertainty in  
223 river models (Hall et al., 2005; Warmick et al., 2010).

## 224 **2.5 Calibration scenarios**

225 The original set of parameters was established by the authors and were not  
226 measurements or calculated values. The hydrodynamic results generated by running the  
227 model with the original set of parameters were then used in the calibration process.  
228 Using the data recorded during the initial run with the original parameters as the  
229 observation values, PEST is expected to progress towards the initial set of parameters.  
230 Fictional parameter values were used by the authors because not enough data for this  
231 study case is available to proceed to a real calibration case. For each calibration  
232 scenarios, the maximum number of iterations allowed is 30 and the parameters can  
233 range from 0.01 to 0.1. The original values of Manning coefficients, along with the  
234 observation values used in the series of calibrations, are presented in table 1. The series  
235 of calibrations is carried out using different settings, with the number of observation  
236 points, their positions and their content varying in each series.

237 The calibration was performed on a IntelCore i5 2,27 GhZ laptop and required on  
238 average 7 iterations and 60 model runs for the simpler cases and 10 iterations and 100  
239 models runs for the more complex cases. Each model run take approximately 1 hour to  
240 complete.

### 241 **2.5.1 Water depths**

242 The first series of calibrations used an increasing number of observation points, only one  
243 per reach, containing only the observed water depths. In the first case, the calibration  
244 points were located close to the middle of the reach; in the second case, the points  
245 were located near the junctions of reaches or close to the boundary conditions. The first  
246 calibration used two observation points, while the subsequent calibration used one  
247 additional point, with a maximum of five (one per reach) in the first scenario and six in  
248 the second scenario.

### 249 **2.5.2 Water depths and velocities**

250 The next series of calibrations also used an increasing amount of observation points  
251 between each trial. In addition to water depths, observation points contained water  
252 velocity measurements: water velocity in the X- and Y- directions and the magnitude of  
253 this velocity. PEST now has access to an increased quantity of information to proceed  
254 with the calibration to explore the extent of adding information to the observation  
255 points. In all cases, the observation points are located near the centre of each reach.  
256 Each calibration process is carried out with identical instructions sets and regulation  
257 parameters and has the same starting values for the initial model run.

### 258 **2.5.3 Sensitivity analysis**

259 The next parts of the calibration series were used for a sensitivity study to observe the  
260 effects of introducing an error in the measured data used in the calibration procedure.  
261 Different scenarios were carried out using two different sets of observation data to aid  
262 in the calibration process, with a variable magnitude of the introduced error.

263 In the first case, the error was applied to the measured depth in a scenario where only  
264 the measured depth was available for the calibration procedure. In the second case, the  
265 same scenario as in the previous case was carried out by adding measured velocity data  
266 to the observation points to verify the advantages of additional information in the  
267 advent of an error in the data. Only the measured depth was subjected to the  
268 introduced error. The third case introduced an error in the model's input flow using all  
269 the available measured data of the observation points (measured depths and velocities).  
270 This scenario reveals the effect of flow overestimation and underestimation on the  
271 calibration. The first series of this case only included the measured depths at the  
272 observation points; the second scenario included all the measured data, i.e., measured  
273 depth and velocities. Again, partial use of the data in the first case was done to evaluate  
274 the benefits of adding additional data to the calibration process to better handle the  
275 possible introduction of error in the data.

## 276 **3 Results and discussion**

277 The results obtained in the different calibration scenarios are presented in this section,  
278 and the difference between the observed and simulated water depths of the entire

279 model for the final calibration scenarios is shown. The results obtained from the  
280 calibration series and sensitivity calibration series are also discussed.

### 281 **3.1 Water depths**

282 The first series of calibrations only used a growing number of observation points  
283 containing the water depth as a means of correspondence between the model output  
284 values and the measured values. At first, only two observation points were supplied; for  
285 each subsequent calibration run, an observation point was added until each reach was  
286 supplied with a measured water depth. Figures 3 to 6 present the calibration results  
287 from the first series of calibrations.

288 Results show that PEST cannot correctly calibrate reaches without having at least one  
289 observation value in the reach, which in this case is the measured water depth. In each  
290 calibration process, the Manning coefficients in the reaches that are not supplied with  
291 an observation point have little or no variation compared to their starting values. From  
292 the observations made in the results, PEST needs to be supplied with at least one  
293 measured depth in a reach to correctly estimate the parameter value. However, PEST  
294 has no difficulty matching measured water depths, when supplied, in only a few model  
295 runs.

296 If, during the calibration process, PEST cannot find a correlation between the variation  
297 of a parameter and the reduction of the objective function, it will abandon further  
298 modification of the said parameter during the present iteration. This results in  
299 parameters that are left at their original values during the calibration process. Reaches



300 that are left with an unvaried Manning coefficient have an influence on the upstream  
301 portion; thus, PEST, in its quest to match the featured values, must compensate for the  
302 unvaried coefficients with an overestimation of the Manning coefficient to reach the  
303 supplied measured value upstream. This is shown in the calibration results, where PEST  
304 could not correctly calibrate the reach 4 parameter when no information was supplied  
305 downstream in reach 3. When an observation point is added to reach 3, PEST can  
306 correctly adjust the Manning coefficients of both this reach and of reach 4.

307 Figure 7 shows the differences between the water depths recorded at the end of the  
308 calibration process using all the observation points and the water depths recorded with  
309 the original parameter values. The differences between the simulated values are very  
310 low considering that almost all the model's water depths are reproduced within a 0.005  
311 m precision. The majority of the higher differences are located in reach 2, which is an  
312 area characterised by small instabilities in the results.

313 Since the low starting values of the Manning coefficient had a negative influence on the  
314 calibration results, the entire calibration series is reinvestigated by reinitialising the  
315 starting values in a range that would be much closer to a suitable estimation done by  
316 any user. This way, the calibration process could begin with starting values that could  
317 resemble a user's estimation.

318 The results obtained show the same result pattern with a much better performance in  
319 the calibration result since the starting values are closer to the original values. Like in  
320 the previous series, the reaches that are not provided with calibration points remain

321 closer to their original values, but results show a positive movement towards the  
322 desired values as more points are added. In reach 3, the relative difference between the  
323 desired value and the calibration value is gradually diminished as additional points are  
324 added to the surrounding reaches. The same improvement is observed at reach 4,  
325 where overestimation caused by reach 3 is gradually reduced and much less  
326 exaggerated, similar to the previous calibration series.

327 Another calibration series was processed by using observation points located on the  
328 frontier of two reaches in the model to explore the “calibration value” of a different  
329 positioning of the observation points. The results showed that points placed on the  
330 frontier of two reaches facilitate only the calibration of the downstream reach; thus,  
331 one point per frontier is needed to obtain a proper calibration of the model. However,  
332 the uncalibrated reaches in this series did not have the overestimation effect upstream  
333 observed in the previous series.

### 334 **3.2 Water depths and velocities**

335 This series of calibrations also used an increasing number of calibration points, centred  
336 in their respective reaches, with additional measurements: each observation point  
337 featured the measured depths, the velocity along the X- and Y-axis, and the velocity  
338 magnitude. Figures 8 to 11 present the calibration results from the series of calibrations  
339 using water depths and water velocities of the observation points. With only two  
340 observation points (figure 8), PEST can find the desired values of 4 out of 5 reaches. The  
341 calibration parameter of reach 5 remained at the starting value, meaning that PEST

342 could not establish a relation between the parameter variation and the reduction of the  
343 objective function.

344 As additional points are included in the calibration, the relative difference between  
345 PEST's suggested values and the desired values is gradually reduced. In fact, the quality  
346 of the adjustment increases faster with the addition of observation points and the  
347 model is calibrated to a satisfying status with less observation points. Additionally,  
348 reaches that do not have measured values to facilitate their parameter calibration can  
349 be estimated to a good level when upstream and downstream reaches contain  
350 calibration information. This is shown in the third calibration (figure 11), where the  
351 middle reach is correctly calibrated even without having any observation values  
352 attached to it. This series shows that less observation points are required to obtain  
353 satisfactory calibration results when the featured points contain more information.

354 Figure 12 shows the differences between the water depths resulting from the  
355 calibration process using all the observation points (water depths and water velocities)  
356 and the water depths recorded with the original parameter values. The differences are  
357 very similar to those of the calibration using only the water depths, with the exception  
358 of reach 2, which contains the majority of the higher differences from the original  
359 values. Compared to the calibrated Manning coefficient obtained in the other reaches,  
360 the value from reach 2 is overestimated, thus resulting in higher but still acceptable  
361 differences between the observed and simulated water depths. In the other reaches,

362 the differences from the simulated water depth values are still within a 0.005 m  
363 precision.

364 The analysis of the results given by the hydrodynamic model shows that multiple points  
365 in the reach 2 area have oscillating results over time, meaning that the final solution  
366 might slightly differ from one simulation to another. The observation point used in this  
367 reach was carefully selected, ensuring that the instabilities in the point's solution were  
368 limited to minor variations. It is suggested that the additional observation values  
369 supplied in reach 2 were still affected by the instabilities met in the area, causing the  
370 parameter overestimation. Gonzalez (2016) also denoted some numerical instabilities in  
371 the modelled results.

372 Next, a sensitivity study is conducted by introducing an error in the measured values to  
373 explore the effects of using erroneous measurements during the calibration process. In  
374 the first calibration series, the error is embedded in the measured water depth of each  
375 observation point, and the calibration process is solely based on these values to  
376 approximate the parameter values. In the second calibration series, the measured water  
377 velocities are added to the observation points, without any errors. In the third series,  
378 the input model flow is varied and no error is introduced in the measured water depths  
379 or velocities.

### 380 **3.3 Sensitivity analysis: water depth only**

381 In the case where the error is introduced in the measured water depths and the  
382 calibration process relies on these values, the repercussions of the calibration error,

383 presented in figure 13, are distributed in a linear fashion. From the previous calibration,  
384 we know that when five observation points containing measured water depths are  
385 supplied, the calibration results are almost perfect. The introduction of errors in the  
386 measured values raises the relative differences by a magnitude that depends on the  
387 surrounding topography of the reach. Portions of the river with floodplains or larger  
388 sections will suffer from more error, especially when the error overestimates the  
389 measured water depth, as it will require a higher friction coefficient to match the said  
390 value. Reach 1 and 2 suffer the most from the error introduction since they are the  
391 portions of the river with the steepest riverbed slopes and have more floodplains. Reach  
392 3 is less affected since the channel is located in a much narrower area surrounded by  
393 steep hills.

#### 394 **3.4 Sensitivity analysis: water depth and speed**

395 This calibration series is executed in the same manner as that of the previous one, with  
396 the additions of measured water velocities to the observation points. No error is  
397 introduced in these additional values. As figure 14 demonstrates, the relative  
398 differences of the calibrated values are lower than those obtained in the previous series.  
399 In this case, the maximum difference obtained is 20%, compared to 57% in the previous  
400 situation. The differences between each parameter in the individual runs of this series  
401 are less scattered, resulting in a flatter graphical display.

402 The most significant drop in relative difference between this series and the previous is  
403 recorded in reach 1, where the maximum recorded value drops down from a range of

404 15% to 47% to an average of 2%. The considerable reduction in relative error in this  
405 reach, which was previously highly sensitive to water depth variations, is the result of  
406 PEST adjusting the calibration parameter by prioritising the measured water velocities  
407 rather than the erroneous water depths. The results show that reaches that are more  
408 oriented toward fitting the measured water velocities rather than the water depths  
409 have the lowest relative error for the resulting calibrated parameter. This is shown in  
410 figure 15, where calibrated parameters with a better fit towards measured water depths  
411 (low relative difference between measured and calculated water depths) are more likely  
412 to be miscalibrated.

### 413 **3.5 Sensitivity analysis: discharge**

414 The next series of calibrations was carried out by introducing an error in the model's  
415 input flow. Both the measured water depths and velocities were used in the calibration  
416 process. Figure 16 shows the results of this series. The left side of the graph shows a  
417 linear relation between error induced in the model's input flow and error in the  
418 calibration parameter. The right portion of the graph presents a much more erratic  
419 relation with the flow augmentation.

420 Again, individual calibration runs that resulted in an accurate match between measured  
421 and calculated water velocities at the expense of matching the measured water depths  
422 are more likely to have more accurate results with the calibration of the Manning  
423 coefficient. Figure 17 shows the distribution of the relative error between the  
424 calibration parameters and the relative error between the observed and simulated

425 water depth values and water velocity values – the relative errors of water velocities are  
426 summed. The Manning-water depth relation is much more concentrated on the left side  
427 of the graph, with a large variation in the relative errors of the Manning coefficient. This  
428 shows that when the calibration process adjusts the Manning coefficients, with a  
429 tendency to match the measured water depth rather than the water velocities, the  
430 calibration results are somehow more unpredictable.

#### 431 **4 Conclusion**

432 This study presents the development of a tool combining PEST, an automatic calibration  
433 program, with the hydraulic model SRH-2D. The tool serves as an easy-to-use set of  
434 forms that can provide a rapid and functional linkage of a model with the automatic  
435 calibration tool. The amount of information required by the user and the user's  
436 interaction with the tool are minimized to provide a rapid preparation of the calibration  
437 process for the project at hand.

438 The tool was applied to the Ha! Ha! river model based on the post-flooding event of  
439 1996, which drastically changed its morphology. The model comprised five reaches,  
440 each represented by a Manning roughness coefficient. An original set of parameters was  
441 used to generate observation values that were then used for multiple calibration series  
442 conducted to assess the effect of different scenarios on the calibration results. The  
443 positions, number and content of the observation points varied in the scenarios to  
444 establish the minimal calibration conditions and common guidelines for the usage of the  
445 tool.

446 The first series of calibrations used a growing number of observation points containing  
447 the measured water depth until each section was supplied with one observation point.  
448 The calibration results were optimal when one observation point was present for every  
449 reach of the model. Reaches without observation points led to miscalibrated  
450 parameters that negatively influenced the calibration of the upstream parameter. This  
451 negative effect on the upstream reach could be corrected by using observation points  
452 that are as far away as possible from the miscalibrated reach.

453 The results from another calibration series, where the measured water velocities were  
454 added to the observation points, showed that fewer observation points are required to  
455 yield satisfactory calibration results. The use of water velocities in the calibration  
456 process, combined with the water depths, indeed proved to be much more effective  
457 when estimating parameter values. Moreover, the additional information significantly  
458 reduced the calibration error when slight errors were introduced in the measure water  
459 depths.

460 A sensitivity analysis also showed that parameters that were calibrated by providing a  
461 better fit between measured and modelled water velocities presented better results.  
462 Indeed, parameters accentuating the concordance of water depths displayed a wide  
463 range of errors compared to velocities based on parameters that had a more predictable  
464 outcome regarding the calibration error.

465 It is suggested that the automatic aspect of the tool should be used to address the  
466 question of uncertainty and equifinality associated with the parameter estimation



467 obtained through the calibration process. Additional scenarios should be tested to  
468 explore the continuity of the model performance or the continuity of the parameter  
469 estimation when the following calibration conditions are changed: parameter starting  
470 values, parameter range, observation values disposition, etc. Additionally, the  
471 calibration process should be revisited using different performance criteria based on a  
472 global evaluation of the modelled results or a subdomain measurement of performance.  
473 Pappenberger et al. (2007) showed that the way of evaluating the model performance in  
474 the calibration process (i.e., objective function) has an impact on the results at different  
475 scales (local or global). Precaution must also be taken when assessing the calibration  
476 process as equifinality can be encountered when multiple sets of parameters may  
477 satisfy the fitting of the observation data (Beven & Freer, 2001; Pappenberger et al.,  
478 2005).

479 Considering the positive results obtained using the current build of O.P.P.S, further work  
480 should be done to include the sediment transport module of SRH-2D in the automatic  
481 calibration process. As of now, PEST does not include the calibration of discontinuous  
482 parameters, which could possibly cause problems considering that sediment transport  
483 parameters include integer-like input values. In this case, the calibration could be  
484 executed in two consecutive motions: the first would calibrate the continuous  
485 parameters; the second, using the calibration results of the continuous parameters,  
486 could iterate through a user-selected range of discontinuous parameters, selecting the  
487 set of parameters giving the best fit.

488 **Acknowledgments**

489 This research was supported in part by a National Science and Engineering Research

490 Council (NSERC) Discovery Grant, application No: RGPIN-2016-06413.

491

492 **References**

- 493 Aquaveo. (2013). *SMS User Manual, Surface-water Modeling System (v11.1)*.
- 494 Bahremand, A., & De Smedt, F. (2010). Predictive Analysis and Simulation Uncertainty of  
495 a Distributed Hydrological Model. *Water Resources Management*, 24(12), 2869-  
496 2880. doi:10.1007/s11269-010-9584-1
- 497 Beven, K., & Freer, J. (2001). Equifinality, data assimilation, and uncertainty estimation  
498 in mechanistic modelling of complex environmental systems using the GLUE  
499 methodology. *Journal of Hydrology*, 249(1), 11-29.
- 500 Boyle, D. P., Gupta, H. V., & Sorooshian, S. (2000). Toward improved calibration of  
501 hydrologic models: Combining the strengths of manual and automatic methods.  
502 *Water Resources Research*, 36(12), 3663-3674.
- 503 Capart, H., Spinewine, B., Yougn, D. L., Zech, Y., Brooks, G. R., Leclerc, M., & Secretan, Y.  
504 (2007). The 1996 Lake Ha! Ha! breakout flood, Quebec: Test data for geomorphic  
505 flood routing methods. *Journal of Hydraulic Research*, 45, 97-109.
- 506 Diaz-Ramirez, J. N., McAnally, W. H., & Martin, J. L. (2012). Sensitivity of Simulating  
507 Hydrologic Processes to Gauge and Radar Rainfall Data in Subtropical Coastal  
508 Catchments. *Water Resources Management*, 26(12), 3515-3538.  
509 doi:10.1007/s11269-012-0088-z
- 510 Doherty, J. (2010). *PEST, Model-Independent Parameter Estimation User Manual : 5th*  
511 *Edition*: Watermark Numerical Computing.
- 512 Duan, Q., Sorooshian, S., & Gupta, V. (1992). Effective and efficient global optimization  
513 for conceptual rainfall-runoff models. *Water Resour. Res*, 28(4), 1015-1031.
- 514 Ellis, R. J., Doherty, J., Searle, R. D., & Moodie, K. (2009). *Applying PEST (Parameter*  
515 *ESTimation) to improve parameter estimation and uncertainty analysis in*  
516 *WaterCAST models*. Paper presented at the 18th World IMACS Congress and  
517 MODSIM09 International Congress on Modelling and Simulation: Interfacing  
518 Modelling and Simulation with Mathematical and Computational Sciences, Cairns,  
519 Australia. <http://mssanz.org.au/modsim09>
- 520 Fabio, P., Aronica, G. T., & Apel, H. (2010). Towards automatic calibration of 2-D flood  
521 propagation models. *Hydrology and Earth System Sciences*, 14(6), 911-924.  
522 doi:10.5194/hess-14-911-2010
- 523 Gonzalez, P. (2016). *Modélisation de la propagation des inondations en zone urbaine*.  
524 (Master), Université de Montréal, École Polytechnique de Montréal.
- 525 Hall, J. W., Tarantola, S., Bates, P. D., & Horritt, M. (2005). Distributed Sensitivity  
526 Analysis of Flood Inundation Model Calibration. *Journal of Hydraulic Engineering*,  
527 131(2), 117-126. doi:10.1061/(ASCE)0733-9429(2005)131:2(117)
- 528 Kim, S. M., Benham, B. L., Brannan, K. M., Zeckoski, R. W., & Doherty, J. (2007).  
529 Comparison of hydrologic calibration of HSPF using automatic and manual  
530 methods. *Water Resources Research*, 43(1), n/a-n/a. doi:10.1029/2006wr004883
- 531 Lai, Y. G. (2008). *SRH-2D version 2: Theory and User's Manual*: U.S. Department of the  
532 Interior Bureau of Reclamation Technical Service Center Denver, Colorado.
- 533 Lai, Y. G. (2009). Two-dimensional depth-averaged flow modeling with an unstructured  
534 hybrid mesh. *Journal of Hydraulic Engineering*, 136(1), 12-23.

- 535 Lavoie, B., & Mahdi T.-F. (2016). Comparison of two-dimensional flood propagation  
536 models: SRH-2D and Hydro\_AS-2D. *Natural Hazards*, 86(3), 1207-1222.  
537 doi:10.1007/s11069-016-2737-7
- 538 McCloskey, G., Ellis, R., Waters, D., & Stewart, J. (2011). *PEST hydrology calibration*  
539 *process for source catchments—applied to the Great Barrier Reef, Queensland*.  
540 Paper presented at the 19th International Congress on Modeling and Simulation,  
541 Perth, Australia.
- 542 McKibbin, J., & Mahdi, T. -F. (2010). Automatic calibration tool for river models based  
543 on the MHYSER software. *Natural Hazards*, 54(3), 879-899. doi:10.1007/s11069-  
544 010-9512-y
- 545 Pappenberger, F., Beven, K., Frodsham, K., Romanowicz, R., & Matgen, P. (2007).  
546 Grasping the unavoidable subjectivity in calibration of flood inundation models:  
547 A vulnerability weighted approach. *Journal of Hydrology*, 333(2), 275-287.
- 548 Pappenberger, F., Beven, K., Horritt, M., & Blazkova, S. (2005). Uncertainty in the  
549 calibration of effective roughness parameters in HEC-RAS using inundation and  
550 downstream level observations. *Journal of Hydrology*, 302(1-4), 46-69.  
551 doi:10.1016/j.jhydrol.2004.06.036
- 552 Pathak, C. S., Teegavarapu, R. S., Olson, C., Singh, A., Lal, A. W., Polatel, C., . . . Senarath,  
553 S. U. (2015). Uncertainty analyses in hydrologic/hydraulic modeling: Challenges  
554 and proposed resolutions. *Journal of Hydrologic Engineering*, 20(10), 02515003.
- 555 Rode, M., Suhr, U., & Wriedt, G. (2007). Multi-objective calibration of a river water  
556 quality model—Information content of calibration data. *Ecological Modelling*,  
557 204(1), 129-142.
- 558 Vidal, J. P., Moisan, S., Faure, J. B., & Dartus, D. (2007). River model calibration, from  
559 guidelines to operational support tools. *Environmental Modelling & Software*,  
560 22(11), 1628-1640. doi:10.1016/j.envost.2006.12.003
- 561 Warmick, J. J., Klis, H. v. d., & Hulscher, M. J. B. S. J. M. H. (2010). *Quantification of*  
562 *uncertainties in a 2 D hydraulic model for the Dutch river Rhine using expert*  
563 *opinions*. Paper presented at the Environmental Hydraulics.

564

565

566 **Figures Captions**

567 **Fig** O.P.P.S. flow chart

568 **Fig 2** Ha!-Ha! river map and model overview

569 **Fig 3** Calibration results using water depths - 2 observation points

570 **Fig 4** Calibration results using water depths - 3 observation points

571 **Fig 5** Calibration results using water depths - 4 observation points

572 **Fig 6** Calibration results using water depths - 5 observation points

573 **Fig 7** Overall water depths differences between original values and calibrated results

574 using 5 observation points

575 **Fig 8** Calibration results using water depths and water velocities - 2 observation points

576 **Fig 9** Calibration results using water depths and water velocities - 3 observation points

577 **Fig 10** Calibration results using water depths and water velocities - 4 observation points

578 **Fig 11** Calibration results using water depths and water velocities - 5 observation points

579 **Fig 12** Overall water depths differences between original values and calibrated results

580 using 5 observation points containing water depths and velocities

581 **Fig 13** Calibration sensitivity against measured water depths only

582 **Fig 14** Calibration sensitivity against measured water depths with additional information

583 to the observation points

584 **Fig 15** Calibration error distribution of calculated water depth error and the summed  
585 error of calculated water velocities

586 **Fig 16** Calibration sensitivity against model input flow using measured water depth and  
587 velocities

588 **Fig 17** Calibration error distribution of calculated water depth error and the summed  
589 error of calculated water velocities

590

591 **Tables**

592 Table 1 Original values of the Manning coefficient and observation values

| Reach number | Manning's coefficient original values | Observation point values |                  |                  |                          |
|--------------|---------------------------------------|--------------------------|------------------|------------------|--------------------------|
|              |                                       | Water depth (m)          | Velocity X (m/s) | Velocity Y (m/s) | Velocity magnitude (m/s) |
| Reach 1      | 0.02                                  | 1.416                    | 1.146            | 0.941            | 1.481                    |
| Reach 2      | 0.028                                 | 2.786                    | -1.231           | 0.902            | 1.528                    |
| Reach 3      | 0.036                                 | 3.551                    | -0.559           | 0.526            | 0.769                    |
| Reach 4      | 0.026                                 | 3.463                    | -0.28            | 0.537            | 0.605                    |
| Reach 5      | 0.032                                 | 3.222                    | -0.215           | 0.367            | 0.425                    |

593

594

# O.P.P.S.

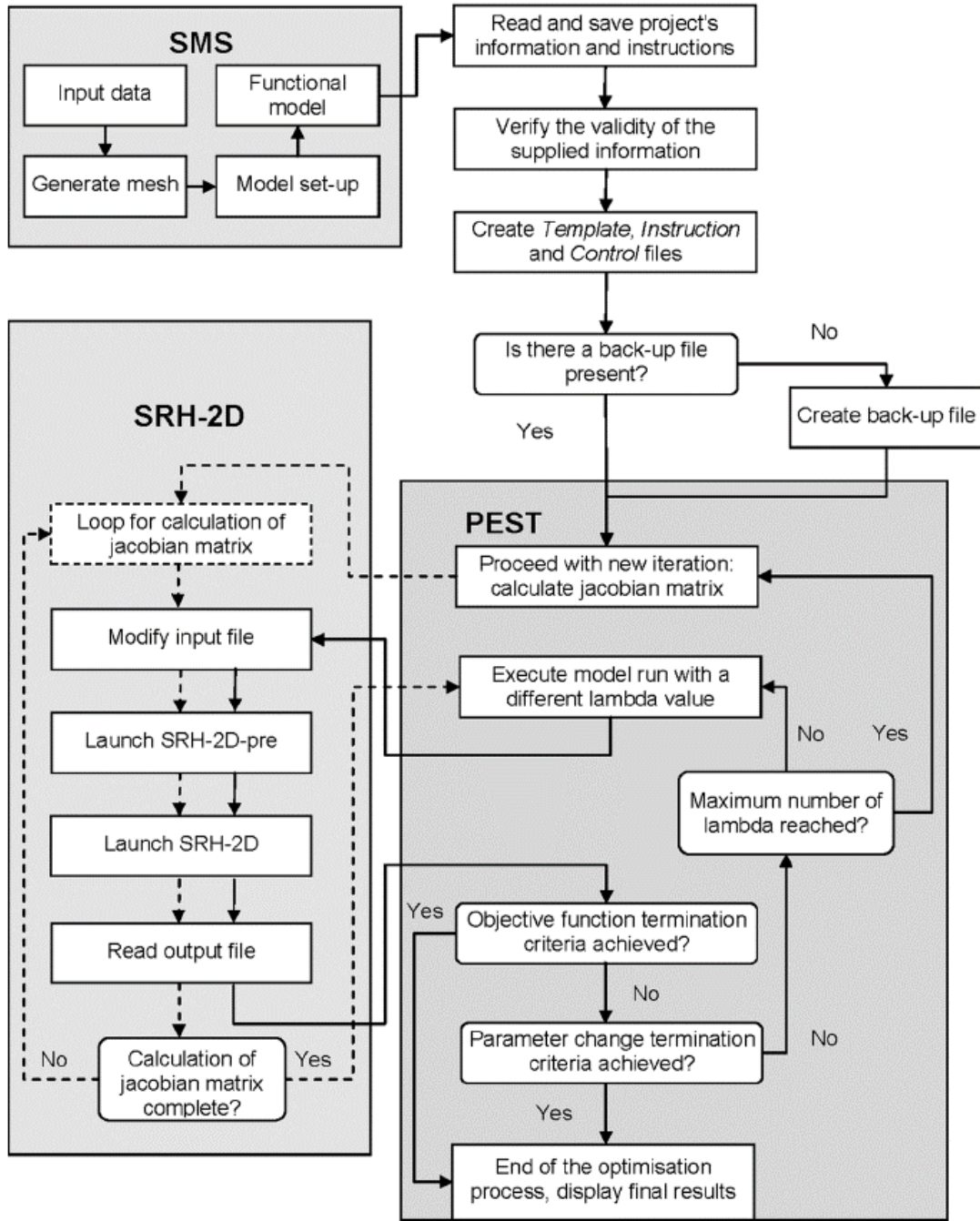
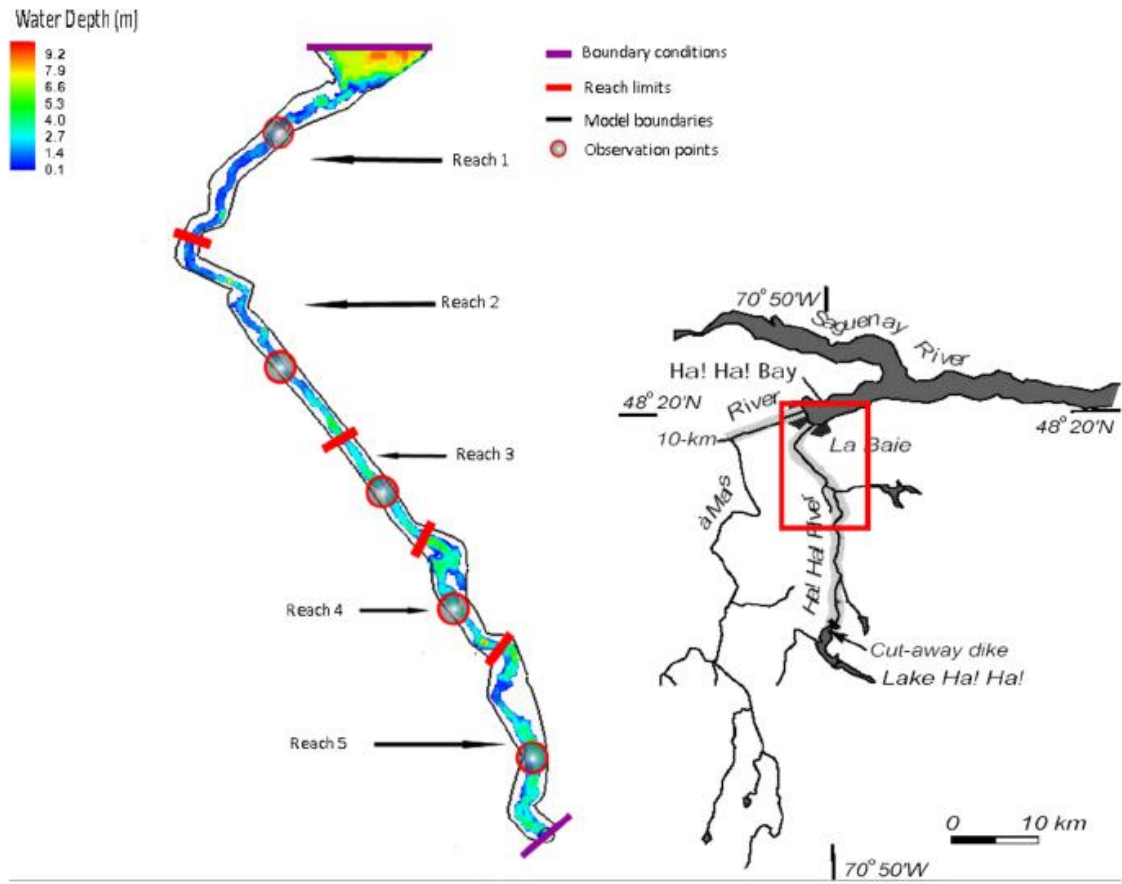


Fig.1 O.P.P.S. flow chart





596

**Fig. 2** Ha!-Ha! river map and model overview

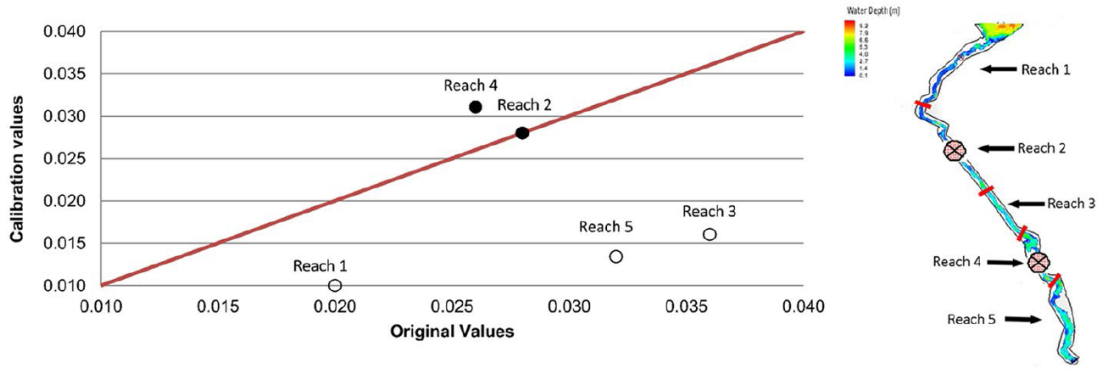


**Fig. 3** Calibration results using water depths—2 observation points

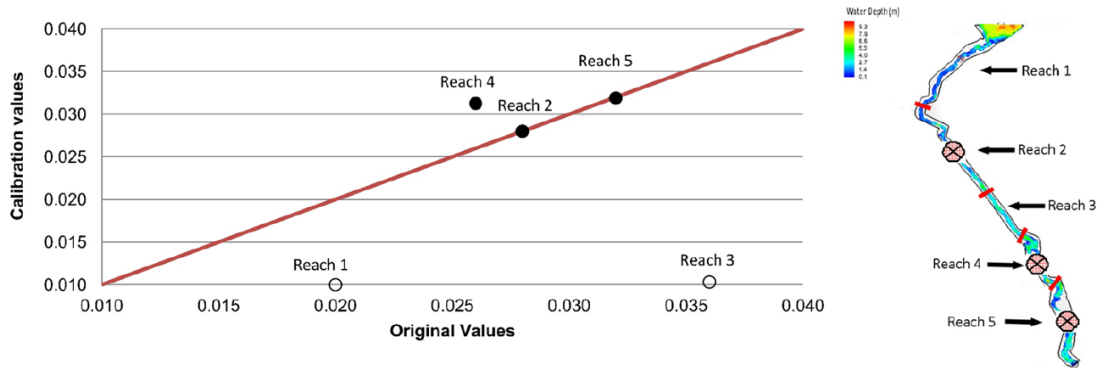


**Fig. 4** Calibration results using water depths—3 observation points

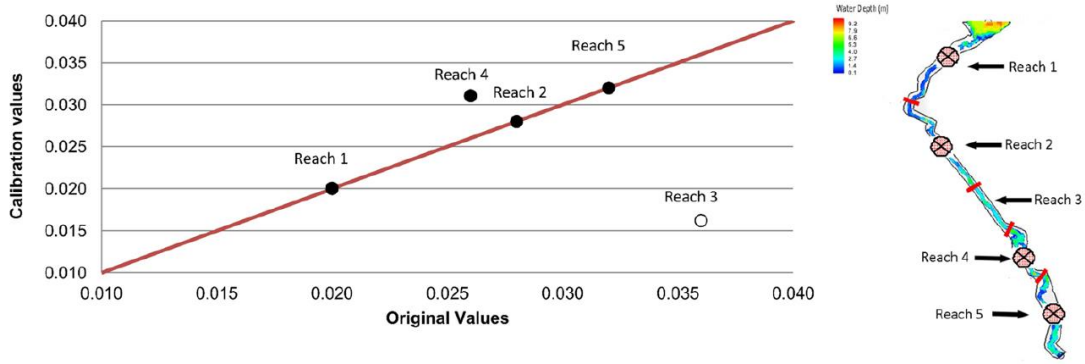


**Fig. 5** Calibration results using water depths—4 observation points

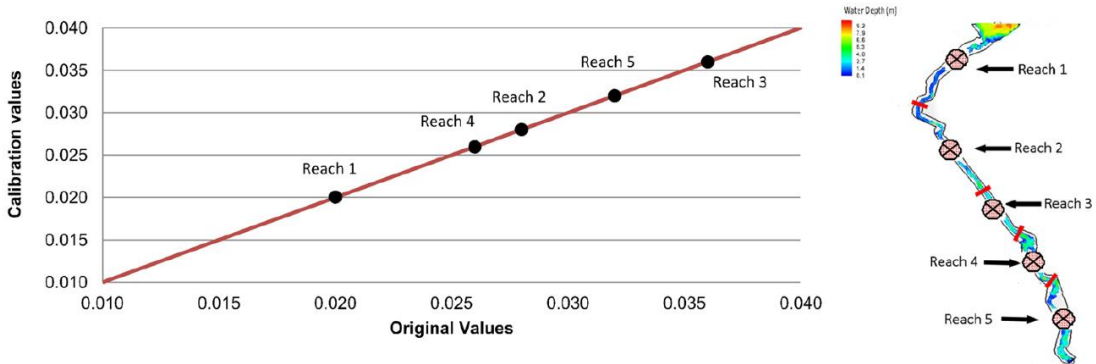
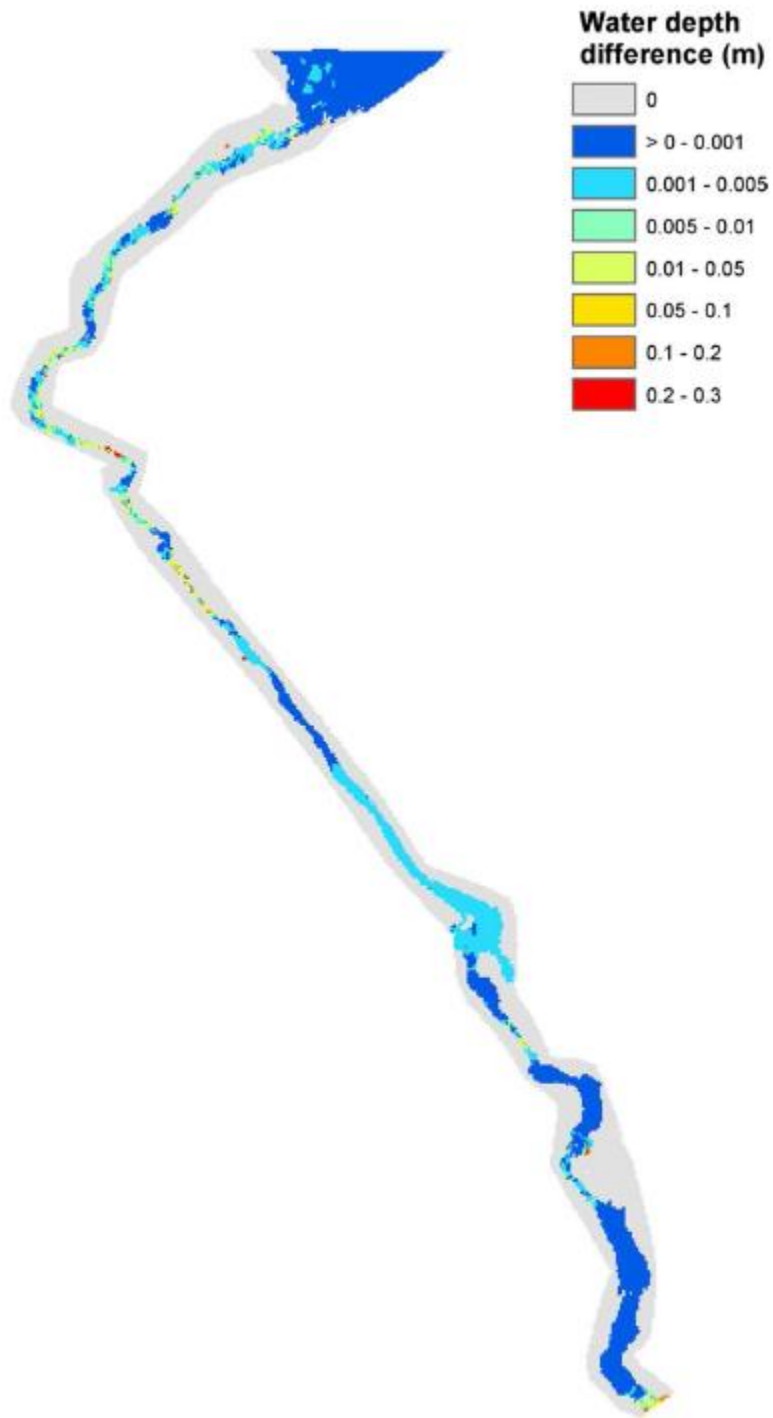


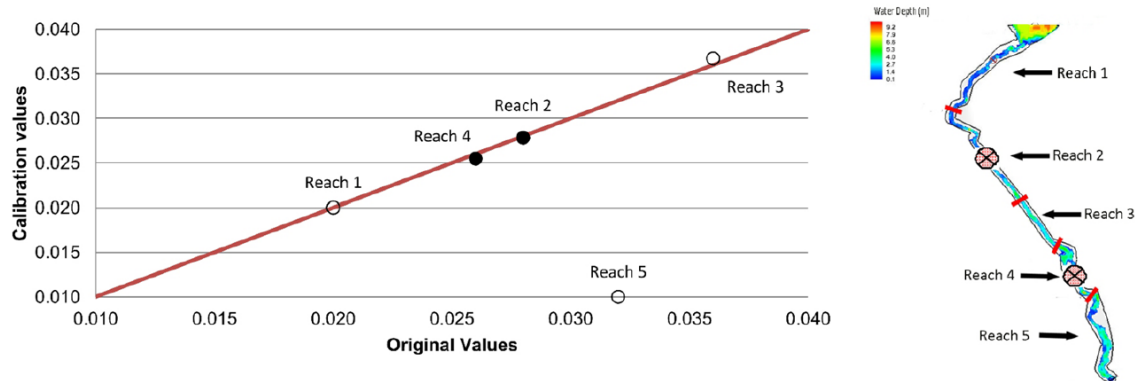
**Fig. 6** Calibration results using water depths—5 observation points



599

600 **Fig 7** Overall water depths differences between original values and calibrated results

601 using 5 observation points



602 **Fig. 8** Calibration results using water depths and water velocities—2 observation points

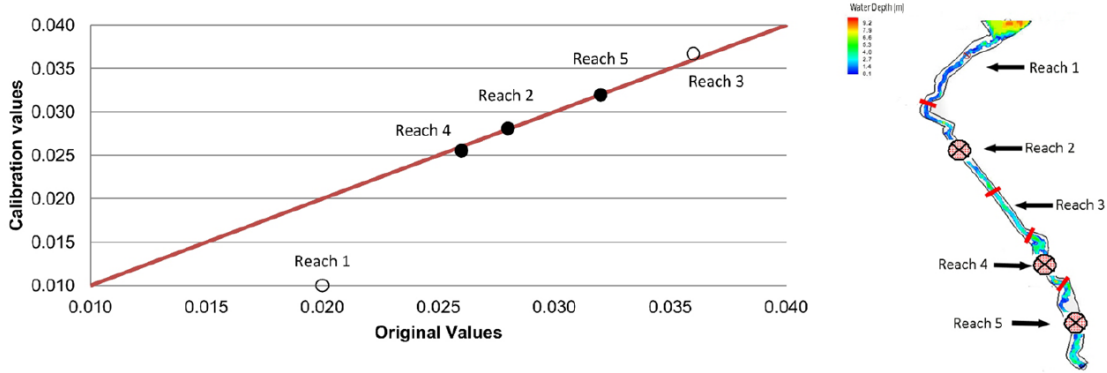


**Fig. 9** Calibration results using water depths and water velocities—3 observation points

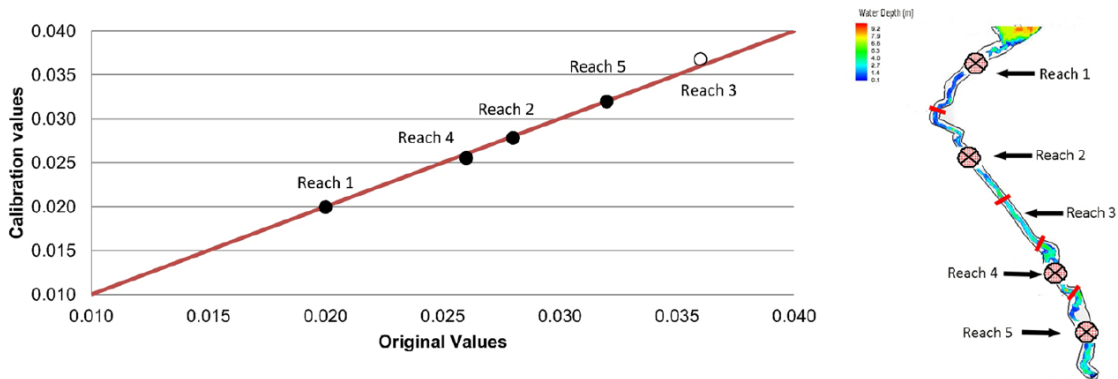


**Fig. 10** Calibration results using water depths and water velocities—4 observation points

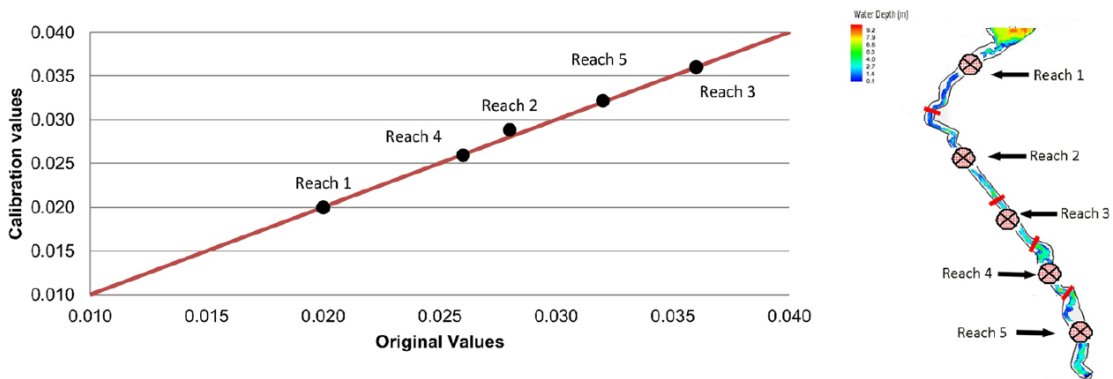
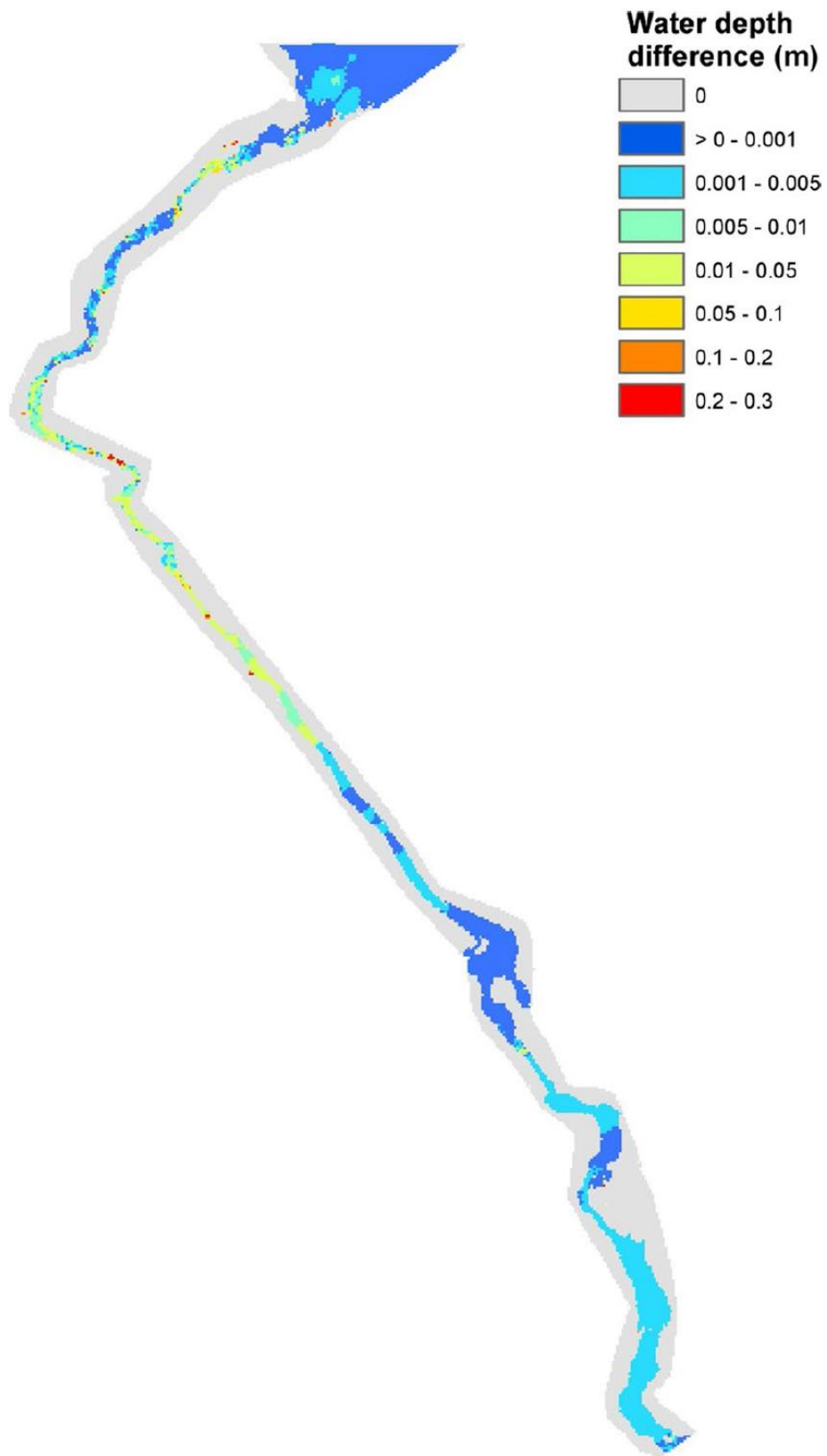
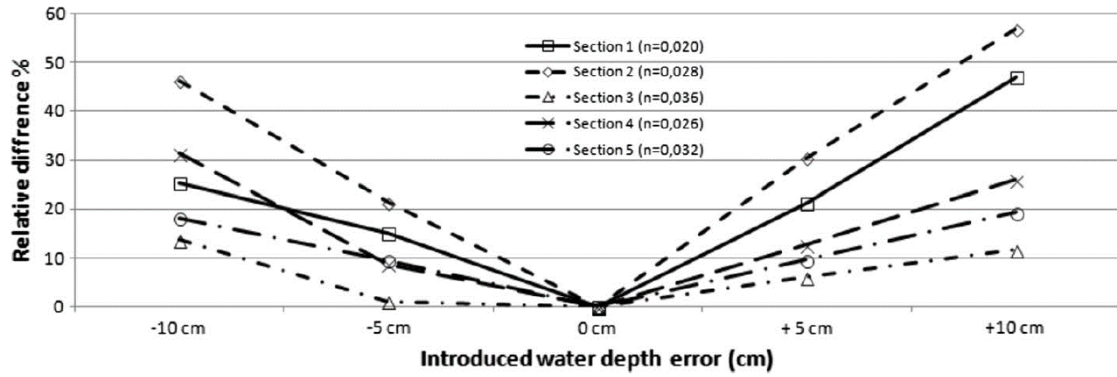


**Fig. 11** Calibration results using water depths and water velocities—5 observation points



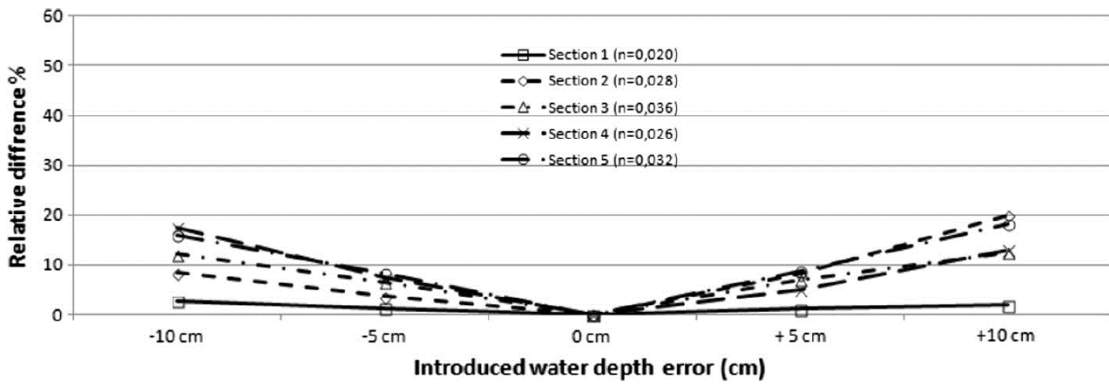
604  
605  
606

**Fig 12** Overall water depths differences between original values and calibrated results using 5 observation points containing water depths and velocities



607  
608

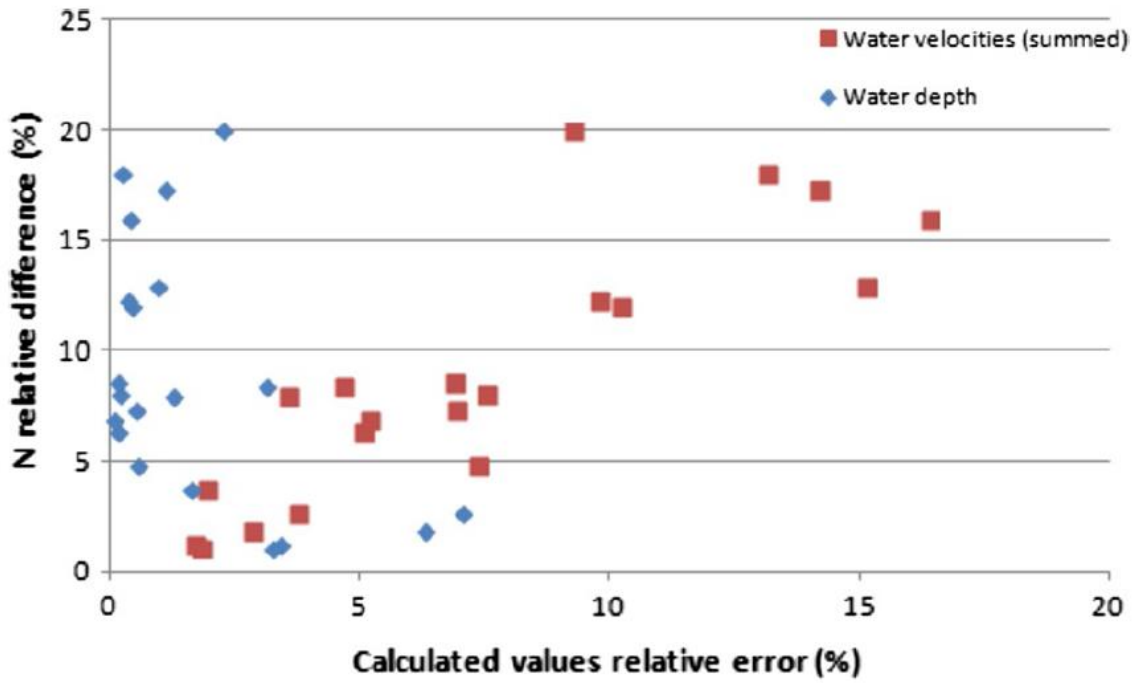
Fig. 13 Calibration sensitivity against measured water depths only



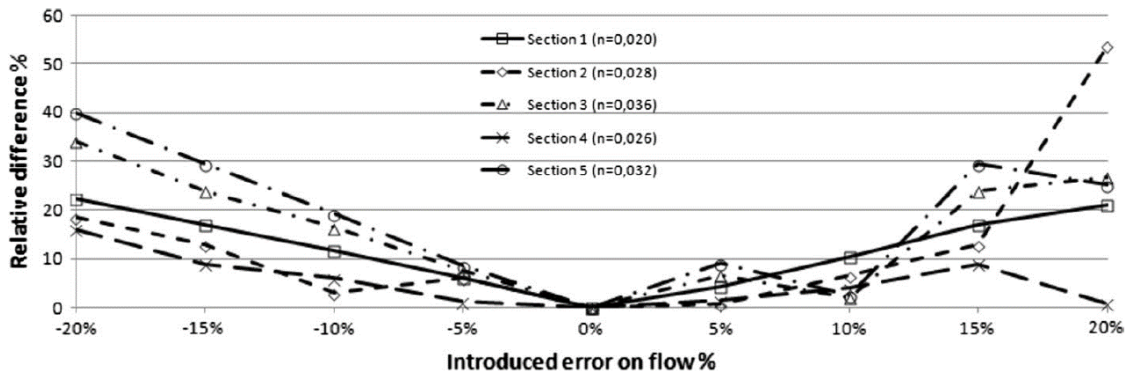
609  
610

Fig. 14 Calibration sensitivity against measured water depths with additional information to the observation points

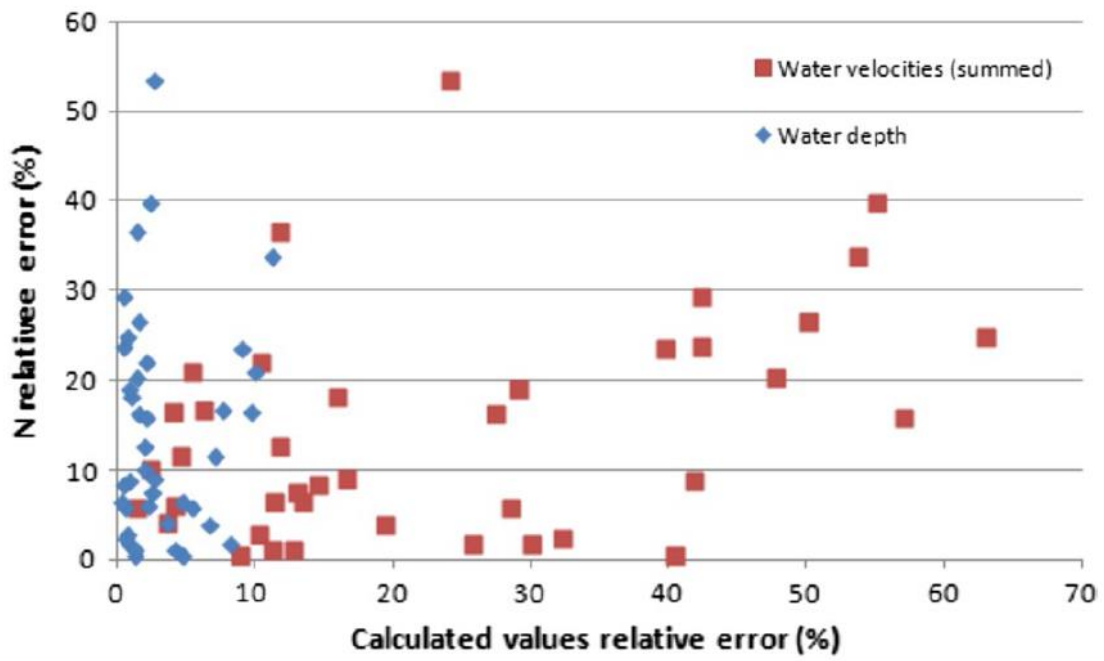




611  
 612 **Fig 15** Calibration error distribution of calculated water depth error and the summed  
 613 error of calculated water velocities  
 614



615 **Fig. 16** Calibration sensitivity against model input flow using measured water depth and velocities  
 616



617  
 618  
 619  
 620

**Fig 17** Calibration error distribution of calculated water depth error and the summed error of calculated water velocities